JOURNAL OF MOLECULAR SPECTROSCOPY 86, 544–554 (1981)

The Far-Infrared Laser Magnetic Resonance Spectrum of the OH Radical

J. M. BROWN, C. M. L. KERR,[1] AND F. D. WAYNE[2]

The Department of Chemistry, Southampton University, Southampton SO9 5NH, England

K. M. EVENSON

National Bureau of Standards, Boulder, Colorado 80302

AND

H. E. RADFORD

Center for Astrophysics, Harvard College Observatory and Smithsonian Astrophysical Observatory, 60 Garden Street, Cambridge, Massachusetts 02138

The far-infrared Laser Magnetic Resonance (LMR) Spectrum of the OH radical in the $v = 0$ level of the $X^2\Pi$ state has been studied in detail. All transitions that are accessible with currently available laser lines have been recorded. The measurements have been analyzed and subjected to a single least-squares fit using an effective Hamiltonian. The data provide primary information on the rotational and fine-structure intervals between the lowest rotational levels and the parameter values determined in the fit are $\tilde{A}_0 = -4168.63913(78)$ GHz, $\tilde{\gamma}_0 = -3.57488(49)$ GHz, $B_0 = 555.66097(11)$ GHz, $D_0 = 0.0571785(86)$ GHz.

1. INTRODUCTION

The hydroxyl radical continues to be an important chemical species. Current interest is centered on its use as a probe of the interstellar environment (*1*) and its involvement in the fundamental steps of chemical reactions (*2*). It is therefore highly desirable to characterize the energy levels of the molecule in the ground $^2\Pi$ state as precisely as possible. Various spectroscopic experiments have been performed with this object in mind. For example, the early work on the microwave spectrum (*3*), later refined in some elegant molecular beam electric resonance studies (*4*, *5*), has established the Λ-type doubling intervals and magnetic hyperfine structure with great precision. Again, the EPR spectrum has been recorded for several low-lying levels (*6*, *7*) permitting the determination of the fundamental Zeeman parameters. It is therefore rather surprising that the two primary parameters for the $X^2\Pi$ state, namely, the spin–orbit coupling constant A and the rota-

[1] Present address: The Herzberg Institute of Astrophysics, The National Research Council, 100 Sussex Drive, Ottawa, Canada K1A OR6.

[2] Present address: Shell Research Ltd., Thornton Research Centre, P.O. Box No. 1, Chester, CH1 3SH, England.

0022-2852/81/040544-11$02.00/0

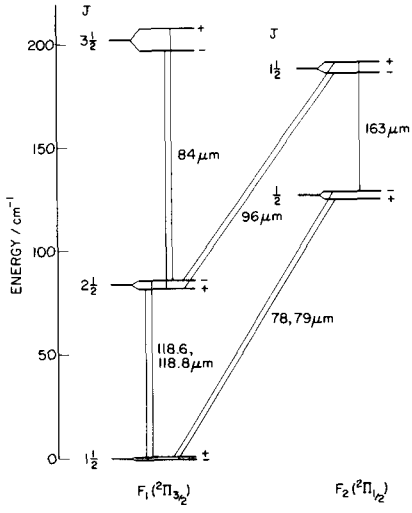

FIG. 1. Diagram showing the lowest energy levels of OH in the $X^2\Pi$ state, and the transitions involved in the far-infrared LMR spectrum. The Λ-type (parity) doubling has been exaggerated by a factor of 20 for clarity.

tional constant B are, by contrast, only poorly determined. For many years, the best available values have been those derived from the optical data of Dieke and Crosswhite (*8*).

A typical separation between the levels of the $X^2\Pi$ state which determine these parameters corresponds to a quantum in the far-infrared region of the spectrum. It is therefore possible to determine A and B by laser magnetic resonance (LMR) spectroscopy at these wavelengths, provided the requisite near-coincidence between the laser and molecular transition frequencies exists. Indeed, OH was one of the first free radicals to be studied by this technique (*9*), using the 79-μm line of the H_2O discharge laser. Mizushima (*10*) has published an analysis of this spectrum. The aim of the present work has been to record and analyze the LMR spectrum of OH, using all available laser lines. In the process, we established as complete a tabulation of the lines in the far-infrared LMR spectrum of OH as possible (Section 2). The measurements are analyzed in terms of an effective Hamiltonian to determine the appropriate molecular parameters for OH in its ground state in Section 3, and the results are discussed in Section 4.

While this work was in progress, Coxon (*11*) reanalyzed the available frequencies in the $A^2\Sigma^+-X^2\Pi$ system of OH in conjunction with the microwave frequencies (*4*, *5*) and the infrared emission spectra (*12*) to determine an improved set of parameters for OH in the levels $v = 0-5$ of the ground state. Our results for $v = 0$ compare favorably with his but they are more precise, being direct determinations of the parameters concerned.

2. EXPERIMENTAL DETAILS AND RESULTS

The LMR spectra of the OH radical were recorded on instruments at the National Bureau of Standards, Boulder, Colorado and at the Center for Astrophysics,

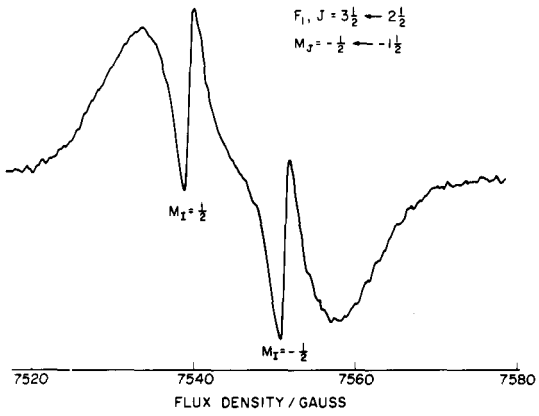

FIG. 2. A line in the 84-μm LMR spectrum of the OH radical. The observation of Lamb dips in this spectrum allow the proton hyperfine structure to be resolved.

Cambridge, Massachusetts. Details of both pieces of equipment have been given in earlier publications (*13–15*). The OH radicals were generated by the reaction between H atoms, produced by a discharge in flowing hydrogen gas, and NO_2. The observed signals were very strong. When the total pressure in the sample region was allowed to rise above about 100 mTorr, the absorption of the laser line was strong enough either to extinguish the far-infrared laser or to produce LMR signals which saturated the amplifiers in the detection system. All measurements were made at pressures of a few tens of millitorr.

Five rotational transitions in OH were observed using seven laser lines. The results are summarized on the energy level diagram in Fig. 1, from which it can be seen that four independent rotational spacings are established in this work. At low modulation levels, the observed linewidths (peak to peak separation of the first derivative traces) were between 10 and 100 G (1 G = 10^{-4} Tesla), being determined by the magnetic tuning rates of the interacting M components and Doppler broadening. Sharp saturation (Lamb) dips were observed on lines in the spectra recorded at 84 and 163 μm; a typical example is shown in Fig. 2, where the proton hyperfine structure is resolved from underneath the Doppler profile.

Magnetic flux densities were measured in each case with a proton NMR fluxmeter. After the magnet has been set to the center of the absorption line, the NMR frequency was measured promptly without alteration of the Fieldial setting. The stability of the Fieldial system was checked periodically. The precision of measurement varied from line to line reflecting the differences in tuning rate. For most lines it was between 0.3 and 1.0 G but the high field lines in the 84-μm π spectrum exceeded the operating range of the NMR fluxmeter and were only measured to ± 10.0 G. The laser frequencies, which are given in Table I, were taken from the measurements of Petersen *et al.* (*16*). They are subject to two sources of error. First, there is the error of measurement, 1.0 MHz for the water discharge laser lines and 0.5 MHz for the optically pumped methanol lines. Second, there is the uncertainty caused by resetability and drift of the far-infrared laser from the

TABLE I

Flux Densities and Frequencies of Transitions Observed by LMR for OH in the $X^2\Pi$ State

Parity[a]	M_J'/F'[b]	M_I'/M_F'[b]	M_J	M_I	Flux density (G)	$\nu_{Laser}-\nu_{calc}$[c] (MHz)	Weight (MHz^{-2})
78 μm spectrum (ν_L = 3821771.3 MHz); F_2, J = 1/2 ← F_1, J = 3/2							
⊥ - polarization (σ)							
+	1	0	-3/2	1/2	16457.1	1.5	0.103
+	1	-1	-3/2	-1/2	16481.1	5.3	0.103
+	0	0	-3/2	1/2	16503.5	1.7	0.103
-	-1/2	1/2	-3/2	1/2	18030.8	2.1	0.103
-	-1/2	-1/2	-3/2	-1/2	18046.1	3.3	0.103
∥ - polarization (π) no transitions observed below 24 kgauss							
79 μm spectrum (ν_L = 3790474.5 MHz); F_2, J = 1/2 F_1, J = 3/2							
⊥ - polarization (σ)							
+	1	0	-3/2	1/2	618.9	0.7	0.742
+	1	-1	-3/2	-1/2	640.8	0.0	0.742
+	0	0	-3/2	1/2	665.2	0.1	0.742
+	1	1	-1/2	1/2	1881.0	-0.2	0.963
+	1	0	-1/2	-1/2	1903.7	0.2	0.963
+	0	0	-1/2	-1/2	2041.5	0.1	0.963
-	1/2	-1/2	-3/2	1/2	2182.5	-0.2	0.742
-	-1/2	1/2	-3/2	1/2	2195.1	0.1	0.742
-	-1/2	-1/2	-3/2	-1/2	2210.3	0.3	0.742
-	1/2	1/2	-1/2	1/2	6495.8	-0.6	0.963
-	1/2	-1/2	-1/2	-1/2	6525.4	-0.8	0.963
∥ - polarization (π)							
+	1	0	-1/2	1/2	1870.1	-0.1	0.963
+	1	-1	-1/2	-1/2	1893.1	0.1	0.963
+	0	0	-1/2	1/2	2006.1	0.6	0.963
-	-1/2	1/2	-1/2	1/2	6553.3	1.4	0.963
-	-1/2	-1/2	-1/2	-1/2	6559.9	1.8	0.963
Magnetic dipole transitions, ⊥ polarization (π)							
-	0	0	3/2	-1/2	180	-1.2	0.0
-	1	1	3/2	1/2	207	-1.2	0.0
-	1	0	3/2	-1/2	227	0.3	0.0
84 μm spectrum (ν_L = 3557147.4 MHz); F_1, J = 7/2 ← F_1, J = 5/2							
⊥ - polarization (σ)							
-	-3/2	1/2	-5/2	1/2	5869.2	-0.5	0.915
-	-3/2	-1/2	-5/2	-1/2	5884.6	-0.3	0.915
-	-1/2	1/2	-3/2	1/2	7539.9	-0.4	0.947
-	-1/2	-1/2	-3/2	-1/2	7551.9	-0.4	0.947
-	1/2	1/2	-1/2	1/2	10534.9	0.0	0.972
-	1/2	-1/2	-1/2	-1/2	10540.3	0.1	0.972
+	-3/2	1/2	-5/2	1/2	13167.2	0.9	0.915
+	-3/2	-1/2	-5/2	-1/2	13182.0	0.8	0.915

[a] Parity of lower state.

[b] Primed quantum numbers refer to the upper state. Half-integral values M_J, M_I apply for the nuclear spin-decoupled representation, and integral values F, M_F for the spin-coupled representation.

[c] Calculated frequency obtained using the parameter values from Table II.

center of its Doppler-broadened gain curve during the course of an experiment. This is variously estimated to be between 0.3 and 1.0 MHz.

We have also searched unsuccessfully for the LMR spectra of OH with other

TABLE I—*Continued*

Parity[a]	M_J'/F'[b]	M_I'/M_F'[b]	M_J	M_I	Flux density (G)	$\nu_{Laser}-\nu_{calc}$[c] (MHz)	Weight (MHz^{-2})
+	-1/2	1/2	-3/2	1/2	16901.6	0.3	0.947
+	-1/2	-1/2	-3/2	-1/2	16912.1	0.2	0.947
-	3/2	-1/2	1/2	-1/2	17449.3	0.7	0.990
-	3/2	1/2	1/2	1/2	17461.3	-0.1	0.990
|| - polarization (π)							
-	-5/2	1/2	-5/2	1/2	10635.0	-0.9	0.963
-	-5/2	-1/2	-5/2	-1/2	10663.6	-0.9	0.963
-	-3/2	1/2	-3/2	1/2	17788.0	4.2	0.082
-	-3/2	-1/2	-3/2	-1/2	17818.0	3.9	0.082
96 μm spectrum (ν_L = 3105936.8 MHz); F_2, J = 3/2 ← F_1, J = 5/2							
⊥ - polarization (σ)							
+	3/2	1/2	5/2	1/2	2524.4	4.6	0.122
+	3/2	-1/2	5/2	-1/2	2524.4	1.8	0.122
-	3/2	-1/2	5/2	-1/2	3413.8	2.8	0.244
-	3/2	1/2	5/2	1/2	3434.5	4.9	0.244
+	1/2	1/2	3/2	1/2	4497.4	3.1	0.342
+	1/2	-1/2	3/2	-1/2	4497.4	-1.0	0.342
-	1/2	-1/2	3/2	-1/2	6100.9	-4.0	0.683
-	1/2	1/2	3/2	1/2	6111.0	-2.8	0.683
|| - polarization (π)							
+	3/2	1/2	3/2	1/2	3842.5	-4.9	0.262
+	3/2	-1/2	3/2	-1/2	3842.5	-6.7	0.262
-	3/2	-1/2	3/2	-1/2	5199.6	0.2	0.523
-	3/2	1/2	3/2	1/2	5233.0	-0.8	0.523
118.6 μm spectrum (ν_L = 2527952.0 MHz); F_1, J = 5/2 ← F_1, J = 3/2							
⊥ - polarization (σ)							
+	-1/2	1/2	-3/2	1/2	8378.4	0.7	0.808
+	-1/2	-1/2	-3/2	-1/2	8402.1	0.9	0.808
-	-1/2	1/2	-3/2	1/2	11057.1	1.9	0.808
-	-1/2	-1/2	-3/2	-1/2	11080.8	1.4	0.808
+	1/2	1/2	-1/2	1/2	13632.3	0.8	0.738
+	1/2	-1/2	-1/2	-1/2	13649.4	1.0	0.738
-	1/2	1/2	-1/2	1/2	17933.4	-0.3	0.738
-	1/2	-1/2	-1/2	-1/2	17947.3	2.0	0.738
|| - polarization (π)							
+	-3/2	1/2	-3/2	1/2	14382.4	0.4	0.917
+	-3/2	-1/2	-3/2	-1/2	14416.8	0.6	0.917
-	-3/2	1/2	-3/2	1/2	19012.0	5.1	0.111
-	-3/2	-1/2	-3/2	-1/2	19048.0	4.6	0.111

laser lines. Calculations suggest that there are suitable near-coincidences between the $J = 5\frac{1}{2} \leftarrow 6\frac{1}{2}$, $F_2 \leftarrow F_1$ transition and the 181.9-μm laser line (N_2H_4) and between the $J = 6\frac{1}{2} \leftarrow 7\frac{1}{2}$, $F_2 \leftarrow F_1$ transition and the 192.9-μm laser line (N_2H_4). However, the transitions are expected to be four to five orders of magnitude weaker than the lines in the 118-μm spectrum, which puts them on the limit of detectability with present sensitivity.

3. ANALYSIS

The assignment of the lines in the LMR spectra was straightforward because, although the electron spin coupling scheme is midway between the Hund's case

TABLE I—*Continued*

Parity[a]	M_J'	M_I'	M_J/F[b]	M_I/M_F[b]	Flux density (G)	$\nu_{Laser}-\nu_{calc}$[c] (MHz)	Weight (MHz^{-2})
118.8 μm spectrum (ν_L = 2522781.6 MHz); F_1, J = 5/2 ← F_1, J = 3/2							
⊥ - polarization (σ)							
+	-1/2	1/2	-3/2	1/2	5194.9	-1.1	0.344
+	-1/2	-1/2	-3/2	-1/2	5218.8	-1.3	0.344
-	-1/2	1/2	-3/2	1/2	7877.6	-1.5	0.344
-	-1/2	-1/2	-3/2	-1/2	7900.9	-1.4	0.344
+	1/2	1/2	-1/2	1/2	8474.6	-1.5	0.800
+	1/2	-1/2	-1/2	-1/2	8491.3	-0.9	0.800
-	1/2	1/2	-1/2	1/2	12805.4	-2.1	0.800
-	1/2	-1/2	-1/2	-1/2	12821.0	-1.7	0.800
∥ - polarization (π)							
+	-3/2	1/2	-3/2	1/2	8920.5	-1.6	0.868
+	-3/2	-1/2	-3/2	-1/2	8954.8	-1.5	0.868
-	-3/2	1/2	-3/2	1/2	13551.1	-2.1	0.868
-	-3/2	-1/2	-3/2	-1/2	13586.2	-2.0	0.868
163 μm spectrum (ν_L = 1838839.3 MHz); F_2, J = 3/2 ← F_2, J = 1/2							
⊥ - polarization (σ)							
-	-3/2	1/2	0	0	3511.4	0.2	3.89
-	-3/2	-1/2	1	-1	3647.8	-0.7	3.89
-	-3/2	1/2	1	0	3834.9	0.2	3.89
-	-1/2	-1/2	0	0	9775.2	0.1	3.99
-	-1/2	-1/2	1	0	10697.2	0.5	3.99
-	-1/2	1/2	1	1	10903.1	2.4	3.99
-	-1/2	1/2	1	-1	14479.0	-0.9	2.34
∥ - polarization (π)							
-	-1/2	1/2	0	0	10394.1	0.1	3.99
-	-1/2	-1/2	1	-1	11137.5	-1.8	3.96
-	-1/2	1/2	1	0	11358.5	0.6	3.96

(a) and (b) for the levels involved, the Zeeman effect can be reliably described by the first-order formula

$$E = E_0 + g_J \mu_B B_0 M_J, \tag{1}$$

where E_0 is the zero-field energy, g_J is the g factor for level J, μ_B is the Bohr magneton, B_0 is the resonance flux density, and M_J is the quantum number of the component of J along the magnetic field direction. The assignments of J, spin component (F_1 or F_2), parity, and M_J could therefore be made by comparing the observations with the formulae for parallel (π) and perpendicular (σ) transitions:

$$\pi \qquad \nu_L - \nu_0 = (\mu_B B_0/h) M_J''(g_J' - g_J''), \tag{2a}$$

$$\sigma \qquad \nu_L - \nu_0 = (\mu_B B_0/h)[(g_J' - g_J'')M_J'' \pm g_J']. \tag{2b}$$

As usual, the primes and double primes refer to the upper and lower states, respectively; the upper and lower signs in Eq. (2b) refer to transitions with $\Delta M_J = +1$ and -1, respectively. The mismatch between the laser and zero-field frequencies ($\nu_L - \nu_0$) was estimated from the best available parameters (*8*, *10*).

The values used for the g_J factors were taken either from the experimental values or the intermediate coupling case formula given by Radford (*6*).

The assignment of the proton hyperfine structure was made in a similar fashion. The transitions involving the $J = 1/2$ level (F_2 component), namely the spectra recorded at 78, 79, and 163 μm, showed unusual behavior. The $J = 1/2$ state is a unique level and has essentially pure $\Omega = 1/2$ character even in the presence of a magnetic field. Consequently the orbital and spin contributions to the magnetic moment cancel out and the Zeeman effect depends on the smaller g factors. In particular, in the negative parity Λ-doubling component of the $J = 1/2$ level (the upper, f level in Fig. 1), the combined electron orbital and spin magnetic moment is almost exactly cancelled by the proton nuclear magnetic moment. As a result, the nuclear spin remains coupled to the rotational angular momentum **J** even in the presence of large magnetic flux densities ($\sim$10 kG). The nuclear spin "forbidden" transitions, formally $\Delta M_I = \pm 1$, are therefore observed for transitions which involve this level with intensities that are comparable to those of the allowed transitions, see Table I. The accidental nature of this cancellation can be appreciated from the behavior of the molecule in the positive parity component of the $J = 1/2$ level. For this state, the nuclear spin decoupling is quite normal, like that for the higher rotational levels.

It can be seen from Table I that some magnetic dipole transitions were observed at low fields in the 79-μm spectrum with reasonable signal-to-noise ratio ($\sim$10:1). The intensities of these transitions are calculated to be about 600 times weaker than the corresponding electric dipole transitions for the same laser line. Additional magnetic dipole transitions were seen in the σ spectrum in the region of 600 G but we have not been able to make accurate measurements of the resonance flux densities because of interference from the much stronger electric dipole transitions in the π spectrum. This implies that the laser electric field was not polarized exactly perpendicular to the applied magnetic field.

The magnetic resonance data in Table I were fitted simultaneously to the parameters of an effective Hamiltonian with a computer program described in Ref. (*7*). The procedure differs from that used in the analysis of the LMR spectrum of CH (*14*), where independent fits were performed for each laser line. Our fit is therefore more constrained but it should also be more informative. The Hamiltonian used in the present work was modified slightly from that given in Ref. (*7*). The earlier work used a Hamiltonian expanded as a power series in $\mathbf{R}^2$, where **R** is the angular momentum of the bare nuclei. Arguments have recently been presented (*17*) suggesting that it is preferable to expand the Hamiltonian as a power series in $\mathbf{N}^2$, where **N** is the resultant of the nuclear and electronic orbital angular momenta. We have followed this recommendation and modified the program accordingly. For the present purposes the only major change involves the rotational constant B; the value for B from a fit to the $\mathbf{N}^2$ Hamiltonian is larger than that obtained from a fit to $\mathbf{R}^2$ Hamiltonian by $2D$. The resonances in the LMR spectrum depend on a large number of molecular parameters. However, several of them have been more accurately determined in other studies and we have constrained these parameters in the least-squares fit. This applies particularly to the Λ-doubling parameters, determined by the molecular beam work (*4*, *5*) and the g factors,

TABLE II

Parameters for OH in the $v = 0$ Level of the $X^2\Pi$ State[a]

(A) Parameter values constrained in the least-squares fit[b]

$10^2\ H$	0.4236[c]	γ_D	0.7315[c]
p	7053.09846	q	-1159.991650
p_D	-1.550962	q_D	0.4420320
$10^3\ p_H$	0.1647	$10^4\ q_H$	-0.8237
a	86.1116	$10\ a_I$	-0.9971
b_F	-73.2537	$10^2\ a_I'$	0.643
c	130.641	$10\ d_D$	-0.2276
d	56.6838		
g_L'	1.00107	$10^3\ g_r$	-0.634
g_S	2.00153	$10^2\ g_\ell'$	0.6386
$10^2\ g_\ell$	0.399	$10^2\ g_r^e'$	0.20443

(B) Parameter values determined in the least-squares fit

$\tilde{A}$[d]	-4168639.13(78)[e]	B	555660.97(11)
$\tilde{\gamma}$[d]	-3574.88(49)	D	57.1785(86)

[a] Values in MHz, where appropriate.

[b] Reference (*7*), unless indicated. Note that the values quoted have been determined from a fit to a Hamiltonian expanded in powers of $\underline{N}^2$, ref. (*17*).

[c] Coxon (*11*).

[d] Effective parameter. The fit was performed with the parameter A_D constrained to zero (*17*).

[e] The numbers in parenthesis represent one standard deviation of the least-squares fit, in units of the last quoted decimal place.

determined from the EPR measurements (*6*, *7*). The values adopted for these parameters are given in Table II. They differ slightly from those given earlier in Ref. (*7*) because the data have been refitted to an N^2 Hamiltonian.

The basis set was truncated without loss in accuracy at matrix elements with $\Delta J = \pm 1$. Each datum was weighted in the fit, inversely as the square of the experimental uncertainty. The latter was estimated as described in Section 2 and the corresponding weights are given in Table I. The primary quantities determined by the data are the rotational and fine-structure intervals shown in Fig. 1. We have chosen to fit these with the four leading parameters $\tilde{A}$, $\tilde{\gamma}$, B, and D and the values determined are given in Table II. The quality of fit is satisfactory as can be judged from the residuals in Table I; the standard deviation of fit relative to the experimental uncertainty is 1.36.

4. DISCUSSION

The rotational and fine-structure parameters for OH determined in this work are in reasonable agreement with those obtained independently by Coxon (*11*), al-

though they are much more precise. Coxon's values, converted to the N^2 formalism for comparison, are

$$\tilde{A}_0 = -4168735(20)\ \text{MHz}, \qquad B = 555661.3(10)\ \text{MHz},$$
$$\tilde{\gamma}_0 = -3594.3(50)\ \text{MHz}, \qquad D = 57.2249(60)\ \text{MHz},$$

where the figures in parenthesis represent one standard deviation of his fit. It is obviously desirable to incorporate the present results in a weighted fit of all the available data, as Coxon has done, to obtain the best set of parameters for OH. An analysis of the 79-μm spectrum similar to the present work has already been performed by Mizushima (*10*). It is difficult to make a comparison with his results because of differences in the Hamiltonian used in his analysis. However, we believe that the present results are an improvement over his work, if only because they involve a much larger data set.

There is a well-established indeterminacy in the effective Hamiltonian for a molecule in a $^2\Pi$ state involving the parameters γ and A_D (*18*). In this work, we have avoided the difficulty by constraining the parameter A_D to zero in the fit; to this extent, the values of the parameters obtained, especially those for $\tilde{A}$ and $\tilde{\gamma}$, are effective values. Brown and Watson (*19*) have shown that it is possible to separate A_D and γ by use of isotopic relationships but the corresponding values for OD, say, are not yet available (although work is in progress on the fitting of the EPR and LMR spectra (*20*) of OD). Coxon (*21*) has estimated the value for A_D of OD in the $v = 0$ level to be -4.36×10^{-4} cm^{-1}. We can therefore use his value with the equation given by Brown and Watson to obtain the following values for OH:

$$\gamma = -3458\ \text{MHz}, \qquad A_D = -24.7\ \text{MHz}.$$

The reliability of these numbers may not be very high, depending directly as they do on Coxon's estimate. However, it can be seen that the parameter γ makes a much larger contribution to $\tilde{\gamma}$ than does A_D. It is therefore preferable to constrain A_D to zero in the fit of data for a single isotope rather than γ; the effective parameters obtained in this case are closer to the "true" values and are hence more meaningful.

The 119-μm transitions of OH ($J = 5/2, F_1 \leftarrow J = 3/2, F_1$) have been detected very recently in a source near the galactic center by Storey *et al.* (*22*). For a comparison with this and similar astrophysical observations, we have computed the zero-field term values of the levels involved in the present work, using the best fit parameters given in Table II. The term values are given in Table III; we estimate that they are reliable to about 3 MHz.

We have attempted to make this work a comprehensive study of the far-ir LMR spectrum of the OH radical. The spectrum is, in fact, quite sparse as can be seen from Fig. 1. There appear to be no other near-coincidences between molecular and laser lines that can be readily exploited for the observation of the molecule in its ground vibrational state. All the measurements have been fitted simultaneously to a single model. The high precision of the data makes this a searching test of the Hamiltonian and the successful conclusion increases confidence in its form. We emphasize the desirability of including all the LMR spectra for a par-

TABLE III

Term Values in Megahertz of Low-Lying Levels of OH in the $v = 0$ Level of the $X^2\Pi$ State

J	F_i	F	+ parity	- parity
$1\frac{1}{2}$	F_1	1	1665.4[a]	0.0
		2	1720.5	53.2
$2\frac{1}{2}$	F_1	2	2509986.9	2516017.7
		3	2510000.9	2516036.0
$\frac{1}{2}$	F_2	0	3786170.4	3790845.6
		1	3786185.3	3790936.0
$1\frac{1}{2}$	F_2	1	5628681.8	5620920.1
		2	5628752.0	5620931.9
$3\frac{1}{2}$	F_1	4	6067223.6	6053782.1
		3	6067224.2	6053789.6

[a]The term values are calculated using the parameter values given in Table II. Their estimated accuracy is 3 MHz.

ticular molecule in a single fit. Ambiguities in assignment or in fitted values can be eliminated and the parameters obtained are more easily interpreted in terms of molecular structure.

ACKNOWLEDGMENTS

We are grateful to the Royal Society of London for the support of C.M.L.K. and to Dr. John Coxon, both for communicating his results before publication and for making helpful comments on an earlier draft of the manuscript. We are also very grateful to Janette Schubert for her valuable work on the computer program.

RECEIVED: September 24, 1980

REFERENCES

1. R. A. BEAUDET AND R. L. POYNTER, *J. Phys. Chem. Ref. Data.* **7**, 311–362 (1978) and references therein.
2. C. J. HOWARD AND K. M. EVENSON, *J. Chem. Phys.* **64**, 4303–4306 (1976) and subsequent papers.
3. G. C. DOUSMANIS, T. M. SANDERS, AND C. H. TOWNES, *Phys. Rev.* **100**, 1735–1754 (1955).
4. W. L. MEERTS AND A. DYMANUS, *Canad. J. Phys.* **53**, 2123–2141 (1975).
5. W. L. MEERTS, *Chem. Phys. Lett.* **46**, 24–28 (1977).
6. H. E. RADFORD, *Phys. Rev.* **122**, 114–130 (1961); **126**, 1035–1045 (1962).
7. J. M. BROWN, M. KAISE, C. M. L. KERR, AND D. J. MILTON, *Mol. Phys.* **36**, 553–582 (1978).
8. G. H. DIEKE AND H. M. CROSSWHITE, *J. Quant. Spectrosc. Radiat. Transfer* **2**, 97–199 (1962).
9. K. M. EVENSON, J. S. WELLS, AND H. E. RADFORD, *Phys. Rev. Lett.* **25**, 199–202 (1970).
10. M. MIZUSHIMA, *Phys. Rev. A* **5**, 143–157 (1972).
11. J. A. COXON, *Canad. J. Phys.* **58**, 933–949 (1980).
12. J. P. MAILLARD, J. CHAUVILLE, AND A. W. MANTZ, *J. Mol. Spectrosc.* **63**, 120–141 (1976).
13. H. E. RADFORD, K. M. EVENSON, AND C. J. HOWARD, *J. Chem. Phys.* **60**, 3178–3183 (1974).

14. J. T. HOUGEN, J. A. MUCHA, D. A. JENNINGS, AND K. M. EVENSON, *J. Mol. Spectrosc.* **72,** 463–483 (1978).
15. F. D. WAYNE AND H. E. RADFORD, *Mol. Phys.* **32,** 1407–1422 (1976).
16. F. R. PETERSEN, K. M. EVENSON, D. A. JENNINGS, J. S. WELLS, K. GOTO, AND J. J. JIMENEZ, *IEEE J. Quantum Electron.* **QE-11,** 838–843 (1975).
17. J. M. BROWN, E. A. COLBOURN, J. K. G. WATSON, AND F. D. WAYNE, *J. Mol. Spectrosc.* **74,** 294–318 (1979).
18. L. VESETH, *J. Mol. Spectrosc.* **38,** 228–242 (1971).
19. J. M. BROWN AND J. K. G. WATSON, *J. Mol. Spectrosc.* **65,** 65–74 (1977).
20. J. S. GEIGER, D. R. SMITH, AND J. D. BONNETT, *Chem. Phys. Lett.* **70,** 600–604 (1980).
21. J. A. COXON, *J. Mol. Spectrosc.* **58,** 1–28 (1975).
22. J. W. V. STOREY, D. M. WATSON, AND C. H. TOWNES, *Astrophys. J.*, in press.